Check for updates

Received: 3 October 2022 | Revised: 15 November 2022 | Accepted: 15 November 2022

DOI: 10.1111/gtc.12993

ORIGINAL ARTICLE

Genes to Cells WILEY

Physiological concentrations of glucocorticoids induce pathological DNA double-strand breaks

Salma Akter[1] | Akihiro Shimba[2,3] | Koichi Ikuta[2] | Md. Rasel Al Mahmud[1] | Shintaro Yamada[1] | Hiroyuki Sasanuma[1] | Masataka Tsuda[1] | Masakatsu Sone[4,5] | Yukio Ago[6] | Kenichi Murai[7] | Hisashi Tanaka[8] | Shunichi Takeda[1,9]

[1]Department of Radiation Genetics, Graduate School of Medicine, Kyoto University, Kyoto, Japan

[2]Laboratory of Immune Regulation, Department of Virus Research, Institute for Frontier Life and Medical Sciences, Kyoto University, Kyoto, Japan

[3]Department of Human Health Sciences, Graduate School of Medicine, Kyoto University, Kyoto, Japan

[4]Department of Metabolic Medicine, Graduate School of Medicine, Kyoto University, Kyoto, Japan

[5]Division of Metabolism and Endocrinology, Department of Internal Medicine, St. Marianna University School of Medicine, Kawasaki, Kanagawa, Japan

[6]Department of Cellular and Molecular Pharmacology, Graduate School of Biomedical and Health Sciences, Hiroshima University, Hiroshima, Japan

[7]Graduate School of Pharmaceutical Sciences, Osaka University, Suita, Osaka, Japan

[8]Department of Surgery, Cedars-Sinai Medical Center, Los Angeles, California, USA

[9]Shenzhen University School of Medicine, Shenzhen University, Shenzhen, Guangdong, China

Correspondence
Shunichi Takeda, Shenzhen University School of Medicine, Shenzhen University, 1066 Xueyuan BLV, Shenzhen, Guangdong, 518060, China.
Email: stakeda@szu.edu.cn

Funding information
JSPS KAKENHI, Grant/Award Numbers: 16H06306, 16H12595, 18H03992, 19H04267, 19K20449, 20K16280, 20K21525, 20KK0186, 21K07148

Communicated by: Akira Shinohara

Abstract

Steroid hormones induce the transcription of target genes by activating nuclear receptors. Early transcriptional response to various stimuli, including hormones, involves the active catalysis of topoisomerase II (TOP2) at transcription regulatory sequences. TOP2 untangles DNAs by transiently generating double-strand breaks (DSBs), where TOP2 covalently binds to DSB ends. When TOP2 fails to rejoin, called "abortive" catalysis, the resulting DSBs are repaired by tyrosyl-DNA phosphodiesterase 2 (TDP2) and non-homologous end-joining (NHEJ). A steroid, cortisol, is the most important glucocorticoid, and dexamethasone (Dex), a synthetic glucocorticoid, is widely used for suppressing inflammation in clinics. We here revealed that clinically relevant concentrations of Dex and physiological concentrations of cortisol efficiently induce DSBs in G_1 phase cells deficient in TDP2 and NHEJ. The DSB induction depends on glucocorticoid receptor (GR) and TOP2. Considering the specific role of TDP2 in removing TOP2 adducts from DSB ends, induced DSBs most likely represent stalled TOP2-DSB complexes. Inhibition of RNA polymerase II suppressed the DSBs formation only modestly in the G_1 phase. We propose that cortisol and Dex frequently generate DSBs through the abortive catalysis of TOP2 at transcriptional regulatory sequences, including promoters or

© 2022 Molecular Biology Society of Japan and John Wiley & Sons Australia, Ltd.

13652443, 0, Downloaded from https://onlinelibrary.wiley.com/doi/10.1111/gtc.12993 by Kyoto University, Wiley Online Library on [14/12/2022]. See the Terms and Conditions (https://onlinelibrary.wiley.com/terms-and-conditions) on Wiley Online Library for rules of use; OA articles are governed by the applicable Creative Commons License

enhancers, where active TOP2 catalysis occurs during early transcriptional response.

KEYWORDS

cortisol, dexamethasone, DNA topoisomerase II, DSB repair, early transcriptional response, glucocorticoid, signal-induced transcription, TDP2/EAPII/TTRAP

1 | INTRODUCTION

Nuclear receptors induce rapid transcriptional responses as transcription factors upon binding to ligands, including androgen, estrogens, and corticosteroids together termed "steroid" hormones. Corticosteroids are produced in the adrenal cortex and include two main classes, glucocorticoids (GCs) and mineralocorticoids. Cortisol is the most crucial GC in the human body and is essential for life (Russell & Lightman, 2019). GCs bind to the glucocorticoid receptor (GR), and ligand-bound GR regulates the transcription of numerous GR-target genes as a transcription factor. GR-mediated signaling suppresses immune cells, and dexamethasone (Dex), a synthetic GC, has been widely used clinically for suppressing immune reactions in patients with allergies, autoimmune diseases, organ transplantations, and COVID-19 (Cain & Cidlowski, 2020; Strehl et al., 2019). Cortisol binds to both GR and mineralocorticoid receptors, whereas Dex binds only to GR (Heming et al., 2018). Dex has ~50 times more potent GR-stimulating activity than the cortisol (Heming et al., 2018). Serum cortisol is at 80–700 nano Molar (nM) (Huang et al., 2007; Scheer et al., 2002), and the clinically relevant concentration of Dex is 6–250 nM (Spoorenberg et al., 2014; Weijtens et al., 1998).

DNA Topoisomerase II (TOP2) plays a vital role in transcriptional responses to various extracellular signals, including nuclear-receptor ligands, cytokines, neurotransmitters, and heat shock (Álvarez-Quilón et al., 2014; Bunch, 2017; Bunch et al., 2014, 2015; Calderwood, 2016; Haffner et al., 2010; Itou et al., 2020; Ju et al., 2006; Madabhushi et al., 2015; McKinnon, 2016; Miyaji et al., 2020; Sano et al., 2008; Wong et al., 2009) (reviewed in [Pommier et al., 2022; Pommier et al., 2016]). TOP2 is also required for the elongation of the transcription (Austin et al., 2018; Joshi et al., 2012; King et al., 2013). There are two TOP2 enzymes (TOP2A and TOP2B), and TOP2A is expressed mainly in cycling cells while TOP2B is ubiquitously expressed (reviewed in [Austin et al., 2018]). TOP2A plays essential roles in DNA replication, decatenation of entangled, newly replicated sister chromatids, as well as condensation of mitotic chromosomes (reviewed in [Nitiss, 2009; Pommier et al., 2016]). TOP2 catalyzes topological changes by strand passage reactions, where one intact double-stranded DNA duplex passes through a transiently formed enzyme-bridged break in the other DNA (gated helix) (reviewed in [Austin et al., 2018; Pommier et al., 2022]). The enzyme-bridged break consists of a TOP2 homodimer covalently bound to the 5′ DNA ends of the break, forming TOP2-DNA cleavage-complex intermediates (TOP2ccs). TOP2 seals TOP2ccs and is released from rejoined genomic DNA.

TOP2 often fails to seal, called "abortive catalysis" (Gómez-Herreros et al., 2014; Hoa et al., 2016; Morimoto et al., 2019; Pommier et al., 2022; Sasanuma et al., 2018; Tubbs & Nussenzweig, 2017), leading to the generation of cytotoxic DSBs called stalled TOP2ccs. Their formation is detectable during early transcriptional responses to nuclear-receptor ligands, heat shock, and insulin at transcriptional regulatory sequences of responding genes (reviewed in [Calderwood, 2016; Madabhushi, 2018; Morimoto et al., 2019; Pommier et al., 2022]). It is controversial whether the generation of stalled TOP2ccs occurs in a programmed fashion with a physiological function or in a stochastic manner (reviewed in [Puc et al., 2017; Morimoto et al., 2019; Pommier et al., 2022]). The latter is supported by the conformational instability of the TOP2 enzyme as both a temperature shift and the HSP90 inhibitor increase the frequency of stalled TOP2cc formation (Karras et al., 2017; Lai et al., 2014).

Re-ligation of stalled TOP2ccs is carried out by coordinated reactions of Tyrosyl-DNA phosphodiesterase 2 (TDP2) and non-homologous end-joining (NHEJ) (Canela et al., 2019; Sciascia et al., 2020). NHEJ requires DNA-dependent protein kinase catalytic subunit (DNA-PKcs) and Ligase IV, which is incapable of joining DSB ends carrying blocking adducts such as 5′ TOP2 adducts (Chappell, 2002; Robins & Lindahl, 1996). TDP2 removes 5′ TOP2 adducts from stalled TOP2ccs before ligation by NHEJ (Cortes Ledesma et al., 2009). TDP2 and BRCA1-MRE11 are complementary to each other in removing 5′ TOP2 adducts (Akagawa et al., 2020; Hoa et al., 2016; Sasanuma et al., 2018), and NHEJ plays the dominant role in DSB repair during G_0/G_1 phases (Ghosh & Raghavan, 2021).

A sex hormone, dihydrotestosterone, causes persistent DSB formation in cells deficient in TDP2 (Al Mahmud et al., 2020; Gómez-Herreros et al., 2014; Sasanuma et al., 2018). Likewise, physiological concentrations of

13652443, 0, Downloaded from https://onlinelibrary.wiley.com/doi/10.1111/gtc.12993 by Kyoto University, Wiley Online Library on [14/12/2022]. See the Terms and Conditions (https://onlinelibrary.wiley.com/terms-and-conditions) on Wiley Online Library for rules of use; OA articles are governed by the applicable Creative Commons License

estrogens are highly genotoxic in cells deficient in either BRCA1, TDP2, or NHEJ, and the genotoxicity is dependent on both estrogen receptors (ERs) and TOP2 (Sasanuma et al., 2018). These data demonstrated the frequent formation of stalled TOP2ccs during the early transcriptional response to the sex hormone. However, GCs are believed to

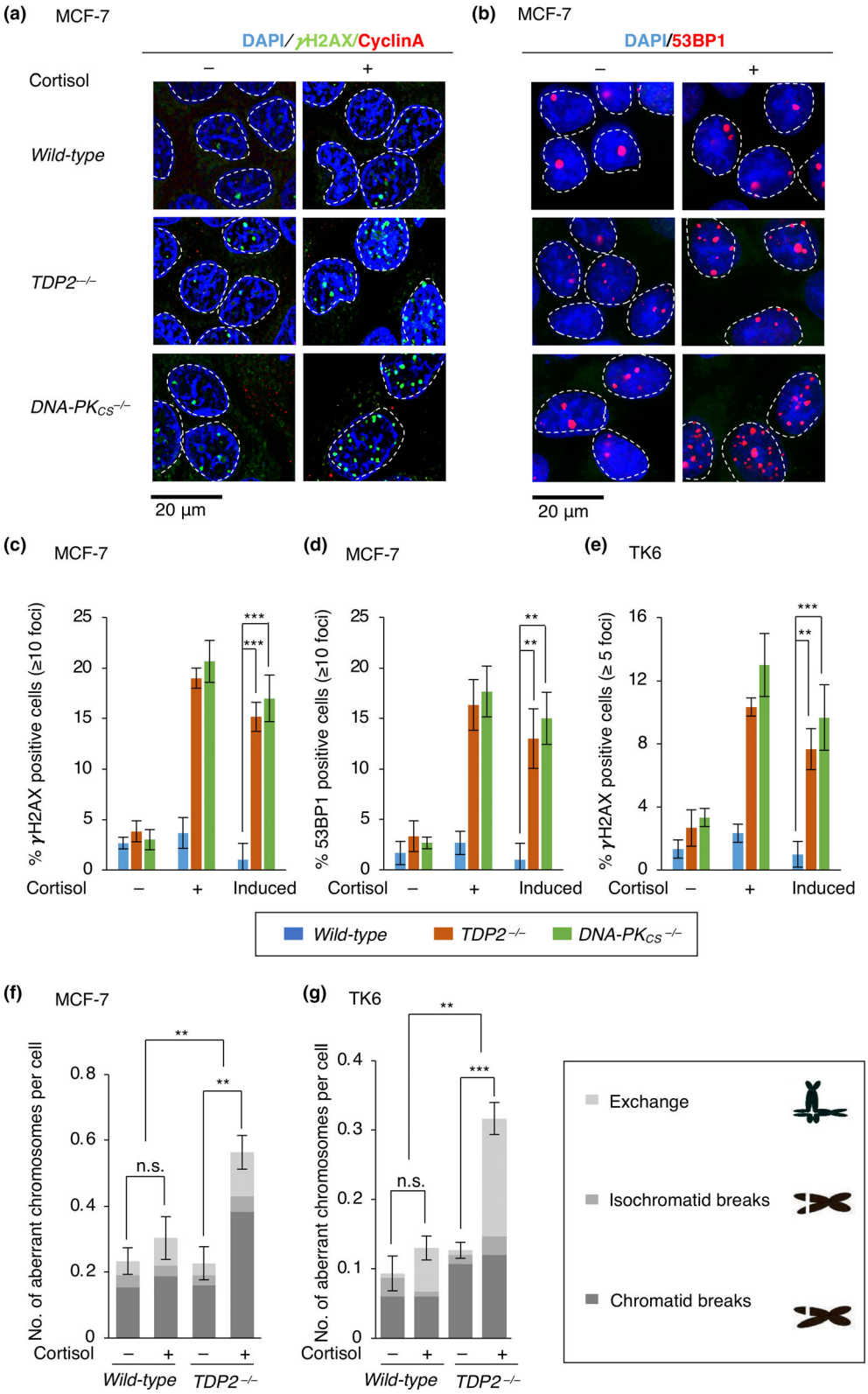

FIGURE 1 Legend on next page.

13652443, 0, Downloaded from https://onlinelibrary.wiley.com/doi/10.1111/gtc.12993 by Kyoto University, Wiley Online Library on [14/12/2022]. See the Terms and Conditions (https://onlinelibrary.wiley.com/terms-and-conditions) on Wiley Online Library for rules of use; OA articles are governed by the applicable Creative Commons License

have no detectable genotoxicity or carcinogenicity (Singh et al., 1994) since they are one of the most widely prescribed drugs. Previous studies poorly studied GC-induced DSBs at serum concentrations.

We here revealed that the exposure of primary lymphoid cells to Dex at a clinically relevant concentration (10 nM) induced one γH2AX focus, the biomarker of individual DSBs, per cell on average, even in the presence of proficient DSB repair. A physiological concentration (100 nM) of cortisol and 10 nM of Dex induced multiple γH2AX foci in each G_1 phase cell deficient in BRCA1, TDP2, or NHEJ. This genotoxicity is dependent on both TOP2 and GR. The inhibition of RNA polymerase II reduced the number of cortisol-induced DSBs only less than 50% in the G_1 phase, which data agree with the estrogen-induced DSBs (Sasanuma et al., 2018). The data suggested the frequent formation of irreversible TOP2ccs at transcriptional regulatory sequences during the early transcriptional response since it involves active TOP2 catalysis at enhancers and promoters (Pommier et al., 2022, 2016). Given continuous exposure of cells in the body to GCs, our data highlights activated GR as the leading endogenous cause of DSBs in genomic DNA.

2 | RESULTS

2.1 | A physiological concentration of cortisol induces DSBs in G_1 phase cells

We explored the induction of DSBs by cortisol in human MCF-7 breast cancer cells and TK6 B lymphoblastoid cells. TK6 has been extensively used by regulatory agencies for identifying the toxicity of industrial chemical products through transcriptome analysis (Buick et al., 2015; Li et al., 2017; Yauk et al., 2016) as well as conventional genotoxic tests (Fellows & O'Donovan, 2010; Gollapudi et al., 2019). To exclude an effect of DNA replication on DSB formation, we examined γH2AX and 53BP1 subnuclear foci, biomarkers for DSBs, only in cyclin-A-negative G_1 phase cells. The cyclin-A-negative cells account for 90% of the serum-starved MCF-7 cells (Sasanuma et al., 2018). The cells we examined in this study are summarized in Table S2. The serum concentration of cortisol in healthy humans is 140–700 nM and 80–350 nM in the morning and midnight, respectively (Huang et al., 2007; Scheer et al., 2002).

We did serum-starvation for 24 h, pulse-exposed *wild-type*, *TDP2*$^{-/-}$, and *DNA-PKcs*$^{-/-}$ MCF-7 cells to 100 nM cortisol for 2 h and measured γH2AX and 53BP1 foci at 2 h after the removal of cortisol (Figure 1a,b and Figure S1). As expected, γH2AX foci were hardly induced by cortisol in *wild-type* cells (Figure 1c and Figure S1). The loss of TDP2 and DNA-PKcs significantly increased the induction of γH2AX foci by cortisol (Figure 1c and Figure S1). The number of 53BP1 foci also increased following exposure of *TDP2*$^{-/-}$ and *DNA-PKcs*$^{-/-}$ cells to cortisol (Figure 1b,d,c and Figure S1). The prominent induction of DSBs by cortisol is also seen in DSB-repair-deficient TK6 cells (Figure 1e and Figure S1d). One hundred nanometre cortisol-induced chromosome breaks in mitotic chromosome spreads in the absence of TDP2 but not in *wild-type* cells (Figure 1f,g). In summary, a physiological concentration of cortisol generates detectable DSBs, and the DSB repair pathway quickly seals them.

FIGURE 1 A physiological serum concentration of cortisol induces DSBs in G_1 cells. (a) Representative images of γH2AX focus formation in G_1-arrested MCF-7 cells following treatment with 100 nM cortisol (+) or solvent (−) for 2 h. After 2 h of cortisol treatment, cells were washed with PBS and further incubated for 2 h with a drug-free medium. Dashed lines indicate outlines of nuclei defined by nuclear DAPI staining. Scale bar, 20 μm. (b) Representative images of cortisol-induced 53BP1 focus formation. Data are shown as in Figure 1a. (c) Fractions of γH2AX-positive cells (≥10 foci per nucleus) following treatment with 100 nM cortisol (+) or solvent (−) in 24 h serum-starved MCF-7 cells. Data are presented as mean ± SD from three independent experiments (100 cells were counted for each replicate). "Induced" was calculated by subtracting the fraction of γH2AX-positive cells in the solvent-treated samples from that in the cortisol-treated samples. SD values for "Induced" were calculated considering the propagation of error. *** $p < .001$ (Student's *t*-test). See also Figure S1 for distributions of γH2AX focus counts per cell for each treatment group. (d) Fractions of 53BP1-positive cells (≥10 foci per nucleus) following treatment with 100 nM cortisol (+) or solvent (−) in 24 h serum-starved MCF-7 cells. Data are shown as in Figure 1c. ** $p < .01$ (Student's *t*-test). See also Figure S1 for distributions of γH2AX focus counts per cell for each treatment group. (e) Fractions of γH2AX-positive TK6 cells (≥5 foci per nucleus) in the cyclin-A-negative. G_1 phase cells after 100 nM cortisol treatment. Data are presented as in Figure 1c. ** $p < .01$, *** $p < .001$(Student's *t*-test). See also Figure S1 for distributions of γH2AX focus counts per cell for each treatment group. (f) Cortisol-induced chromosome aberrations in mitotic chromosome spread of MCF-7 cells. Cells were cultured in the absence (−) and presence (+) of 100 nM cortisol for 36 h. At least 100 mitotic chromosome spreads were analyzed for counting the number of chromatid exchanges, isochromatid breaks (both sister chromatids broken at the same site), and chromatid breaks (one of the two sister chromatids broken) in each experiment. Induced chromosomal breakage significantly increased compared between *wild-type* and *TDP2*$^{-/-}$. Data are presented as mean ± SD from three independent experiments. n.s. = non-significant, ** $p < .01$ (Student's *t*-test). (g) Cortisol-induced chromosome aberrations in TK6 cells. Cells were cultured in the absence (−) and presence (+) of 100 nM cortisol for 15 h. Induced chromosomal breakage significantly increased compared between *wild-type* and *TDP2*$^{-/-}$. Data are presented as in Figure 1f. ** $p < .01$, *** $p < .001$ (Student's *t*-test).

13652443, 0, Downloaded from https://onlinelibrary.wiley.com/doi/10.1111/gtc.12993 by Kyoto University, Wiley Online Library on [14/12/2022]. See the Terms and Conditions (https://onlinelibrary.wiley.com/terms-and-conditions) on Wiley Online Library for rules of use; OA articles are governed by the applicable Creative Commons License

2.2 | A clinically appropriate concentration of Dex induces DSBs at the G_1 phase

We next examined whether Dex induced DSBs at its clinically relevant serum concentration, 6–250 nM (Spoorenberg et al., 2014; Weijtens et al., 1998). We quantified γH2AX foci in serum-starved MCF-7 cells following exposure to 10 nM Dex (Figure 2 and Figure S2). Dex induced γH2AX foci in both *DNA-PKcs*$^{-/-}$ and *TDP2*$^{-/-}$ cells but not in *wild-type* MCF-7 cells at G_0/G_1 phase (Figure 2a and Figure S2). Likewise, Dex induced γH2AX foci in both *DNA-PKcs*$^{-/-}$ and *TDP2*$^{-/-}$ lymphoid cells at cyclin-A-negative G_1 cells (Figure 2b and Figure S2). Like cortisol, Dex-induced chromosome breaks in mitotic chromosome spreads in *TDP2*$^{-/-}$ cells (Figure 2c,d). We conclude that both cortisol and Dex cause DSB formation detectable by the immunocytochemical method in the G_0/G_1 phase. Considering the specific role of TDP2 in removing 5′ TOP2 adducts from DSB ends, DSBs induced by cortisol and Dex most likely represent stalled TOP2ccs.

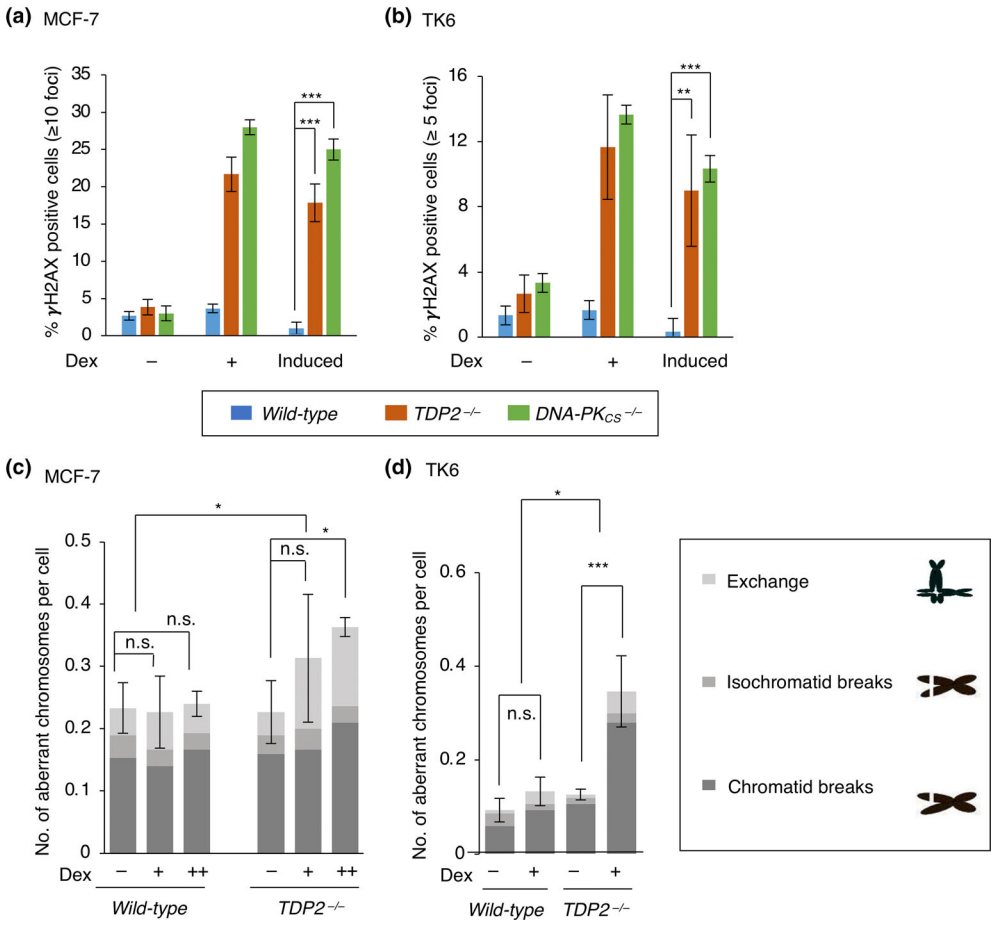

FIGURE 2 Dex induces DSBs in the G_1 phase, and they are rapidly repaired by TDP2 and NHEJ in *wild-type*. (a) Fractions of γH2AX-positive MCF-7 cells (≥10 foci) in the G_1 phase. Cells were treated with 10 nM Dex (+) or ethanol (−). Data are presented as mean ± SD from three independent experiments. γH2AX-foci in at least 100 cells were counted for each replicate. *** $p < .001$ (Student's *t*-test). The increase in the fraction of γH2AX-positive cells following the cortisol treatment (Induced) was calculated as in Figure 1c. See Figure S2 for the distributions of γH2AX focus counts per cell in each treatment group. (b) Fractions of γH2AX-positive TK6 cells (≥5 foci) in the cyclin-A-negative G_1 phase cells after Dex treatment. Data are presented as in Figure 1e. See Figure S2 for the distributions of γH2AX focus counts per cell in each treatment group. ** $p < .01$, *** $p < .001$ (Student's *t*-test). (c) Dex-induced chromosome aberrations in mitotic chromosome spread of MCF-7 cells. Cells were cultured in the absence (−) of Dex, with 10 nM Dex (+), or with 100 nM Dex (++) for 36 h. At least 50 mitotic chromosome spreads were analyzed for counting the number of chromatid exchanges, isochromatid breaks (both sister chromatids broken at the same site), and chromatid breaks (one of the two sister chromatids broken) in each experiment. The same background level of chromosomal breakage (Cortisol [−]) data of WT and TDP2 from Figure 1f are used in Figure 2c. Induced chromosomal breakage significantly increased compared between *wild-type* and *TDP2*$^{-/-}$. Data are presented as mean ± SD from three independent experiments. n.s. = non-significant, * $p < .05$ (Student's t-test). (d) Dex-induced chromosome aberrations in TK6 cells. Cells were cultured in the absence (−) and presence (+) of 10 nM dex for 15 h. The same background level of chromosomal breakage (Cortisol [−]) data of WT and TDP2 from Figure 1g are used in Figure 2d. Induced chromosomal breakage significantly increased compared between *wild-type* and *TDP2*$^{-/-}$. * $p < .05$, *** $p < .001$ (Student's *t*-test). Data are presented as in Figure 2c.

13652443, 0, Downloaded from https://onlinelibrary.wiley.com/doi/10.1111/gtc.12993 by Kyoto University, Wiley Online Library on [14/12/2022]. See the Terms and Conditions (https://onlinelibrary.wiley.com/terms-and-conditions) on Wiley Online Library for rules of use; OA articles are governed by the applicable Creative Commons License

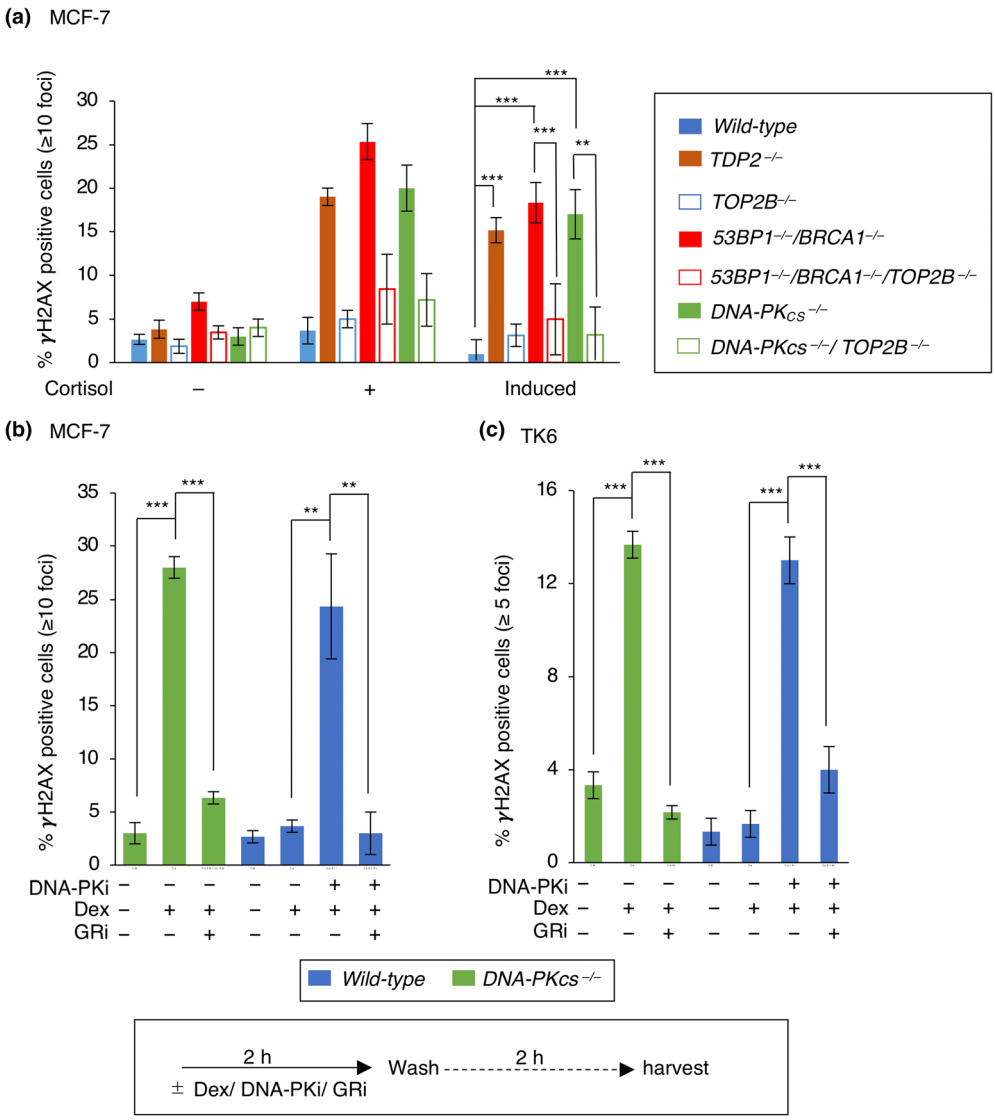

FIGURE 3 Dex-induced DSB formation depends on TOP2B and the glucocorticoid receptor. (a) Serum-starved MCF-7 cells carrying the indicated genotypes were treated with 100 nM cortisol for 2 h and washed. Samples were collected 2 h after the washing of cortisol. Fractions of γH2AX-positive cells were calculated as in Figure 1c. Data are presented as mean ± SD from three independent experiments. γH2AX-foci in at least 100 cells were counted for each replicate. ** $p < .01$, *** $p < .001$ (Student's *t*-test). See Figure S3 for the distributions of γH2AX focus counts per cell (b) *DNA-PKcs*$^{-/-}$ (green) and *wild-type* (blue) MCF-7 cells were treated with 10 nM Dex, 10 μM DNA-PKcs inhibitor (DNA-PKi), and 10 μM glucocorticoid receptor inhibitor (GRi) as shown at the bottom. Dex induced γH2AX foci no decreased after the treatment with GRi. Fractions of γH2AX-positive cells were calculated as in Figure 1c. Data are presented as mean ± SD from three independent experiments. γH2AX-foci in at least 100 cells were counted for each replicate. ** $p < .01$, *** $p < .001$ (Student's *t*-test). (c) *DNA-PKcs*$^{-/-}$ (green) and *wild-type* (blue) TK6 cells were treated as shown at the bottom, and fractions of γH2AX-positive cells were calculated as in Figure 1e. Data are presented as mean ± SD from three independent experiments. γH2AX-foci in at least 100 cells were counted for each replicate. *** $p < .001$ (Student's *t*-test).

2.3 | Induction of DSBs by glucocorticoids requires both TOP2 and GR in G_1 cells

We examined whether TOP2 was required for GC-induced DSBs in MCF-7 cells. TOP2A and TOP2B have substantially overlapping roles in the transcription (Austin et al., 2018; Madabhushi, 2018). The serum starvation of MCF-7 depletes TOP2A more than 20 times (Sasanuma et al., 2018). The serum starvation of *TOP2B*$^{-/-}$ cells provides a unique opportunity to examine the role of TOP2s by inactivating both of them (Figure S3). We analyzed *53BP1*$^{-/-}$*/BRCA1*$^{-/-}$ and *53BP*$^{1-/-}$*/BRCA1*$^{-/-}$*/TOP2B*$^{-/-}$ cells because the former genotype, but not the latter, show the accumulation of estrogen-induced stalled TOP2ccs due to BRCA1-dependent removal of 5′ TOP2 adducts (Sasanuma et al., 2018) (Figure 3a and Figure S3). We also disrupted the *TOP2B* gene in *DNA-PKcs*$^{-/-}$ cells

13652443, 0, Downloaded from https://onlinelibrary.wiley.com/doi/10.1111/gtc.12993 by Kyoto University, Wiley Online Library on [14/12/2022]. See the Terms and Conditions (https://onlinelibrary.wiley.com/terms-and-conditions) on Wiley Online Library for rules of use; OA articles are governed by the applicable Creative Commons License

(Figure S3 and Table S2) and examined GC-induced DSBs in the resulting cells.

We then measured the genotoxic effect of cortisol on *DNA-PK*$^{-/-}$ and *53BP1*$^{-/-}$/*BRCA1*$^{-/-}$ cells, comparing the absence and presence of the *TOP2B* gene in the TOP2A-depleted serum-starved condition (Sasanuma et al., 2018). Like *TDP2*$^{-/-}$ and *DNA-PKcs*$^{-/-}$ cells in Figure 1c, *53BP1*$^{-/-}$/*BRCA1*$^{-/-}$ MCF-7 cells displayed a prominent induction of γH2AX foci following exposure to cortisol (Figure 3a and Figure S3). The loss of TOP2B reduced the median number of cortisol-induced γH2AX foci by around 50% in both *53BP1*$^{-/-}$/*BRCA1*$^{-/-}$ and *DNA-PKcs*$^{-/-}$ cells (Figure S3). γH2AX foci remaining in the absence of TOP2B may result from DSB formation by residual TOP2A. In conclusion, most DSBs induced by cortisol represent stalled TOP2ccs in G_0/G_1.

We next investigated the requirement of GR for the induction of DSBs by Dex, which stimulates only the GR (Heming et al., 2018). We examined the effect of a GR inhibitor (RU-43044) (Morgan et al., 2002) on Dex-induced γH2AX focus formation in *DNA-PKcs*$^{-/-}$ cells and *wild-type* treated with a DNA-PKcs inhibitor (NU7441) (Figure 3b,c). Ten micrometre RU-43044 completely suppressed the induction of γH2AX foci, indicating the requirement of GR for the Dex-dependent induction of DSBs. In conclusion, ligand-bound GR triggers very active catalysis of TOP2, and its abortive catalysis during the transcriptional response generates stalled TOP2ccs, as indicated previously (Morimoto et al., 2019; Puc et al., 2017).

2.4 | Characterization of GC-induced DSBs in primary mouse lymphocytes and human breast cancer cells

To characterize the nature of γH2AX foci, we examined the relationship between the dose of cortisol (Figure 4a–c and Figure S4) and Dex (Figure 4d–f and Figure S4) with the number of induced γH2AX foci in MCF-7 cells at G_0/G_1 phase, thymocytes, and peripheral T cells. To sensitively measure the number of GC-induced γH2AX foci, we examined the freshly prepared primary cells from *wild-type* mice in addition to the cancer cell line for the following reason. The number of spontaneously arising faint γH2AX foci is considerably higher in cancer cell lines than in primary cells (Yu et al., 2006). Accordingly, GC-induced faint γH2AX foci are detectable as GC-induced foci in primary cells but not

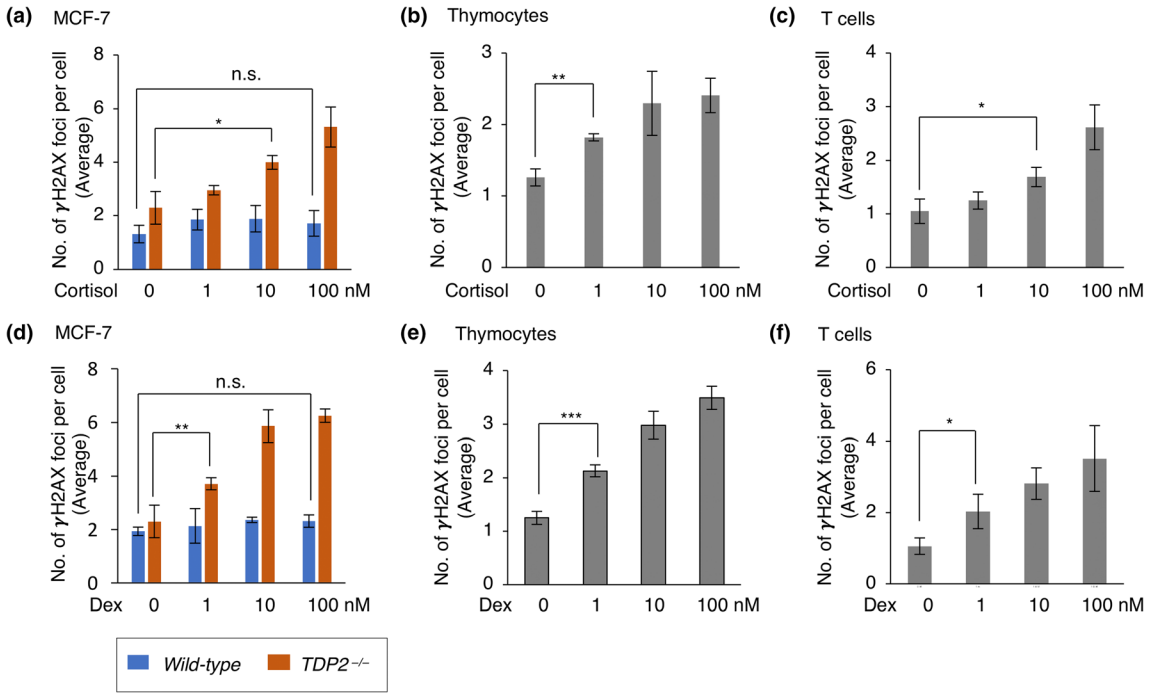

FIGURE 4 1 nM Dex induces DSBs in TDP2-deficient MCF-7 cells and primary murine thymocytes and T cells. Serum-starved MCF-7 cells and thymocytes, and T cells in lymph nodes were treated with the indicated doses of cortisol and Dex. The number of γH2AX foci per cell was counted in three independent experiments. γH2AX-foci in at least 100 cells were counted for each replicate. The average value of each experiment was calculated, and the average of three independent experiments ± SD is presented on Y-axis. * $p < .05$, ** $p < .01$, *** $p < .001$ (Student's *t*-test). (a-c) The average number of γH2AX foci in cortisol-treated MCF-7 cells at G_1 (a), thymocytes (b), and T cells (c). (d-f) The average number of γH2AX foci in Dex-treated MCF-7 cells at G_1 (d), thymocytes (e), and T cells (f). See Figure S4 for the distributions of γH2AX focus counts per cell.

13652443, 0, Downloaded from https://onlinelibrary.wiley.com/doi/10.1111/gtc.12993 by Kyoto University, Wiley Online Library on [14/12/2022]. See the Terms and Conditions (https://onlinelibrary.wiley.com/terms-and-conditions) on Wiley Online Library for rules of use; OA articles are governed by the applicable Creative Commons License

cell lines. When we exposed *TDP2*$^{-/-}$ cells to 1 nM, 10 nM, and 100 nM cortisol and Dex, we found that the number of detectable γH2AX linearly increased (Figure 4a and Figure S4 and Figure 4d and Figure S4). Similarly, the exposure of primary thymocytes and T lymphocytes to 1 nM, 10 nM, and 100 nM GCs caused a linear increase in the number of γH2AX foci (Figure 4b,c,e,f and Figure S4). It should be noted that the low background of γH2AX in these primary cells allows for the sensitive detection of GC-induced DSBs even in DSB-repair-proficient cells. The linear relationship between dose (log scale) and response (γH2AX foci number at a linear scale) agrees with the linear relationship between GC doses and the level of transcriptional response at GC-target genes (Guess et al., 2010).

We characterized Dex-induced γH2AX foci in murine primary thymocytes and peripheral T cells (Figure 5a,b and Figure S5). The addition of DNA-PKcs inhibitor (NU7441) increased the number of Dex-induced γH2AX foci in thymocytes (compare lane 9 with 10 in Figure 5a) and T cells (compare lane 9 with 10 in Figure 5b), indicating that 40% to 50% of the Dex-induced DSBs are repaired by NHEJ. The GR inhibitor completely suppressed Dex-induced DSBs (lanes 4 and 8 in Figure 5a,b). Collectively, 10 nM Dex generates detectable DSBs, most likely stalled TOP2ccs, in a GR-dependent manner in primary lymphocytes and human breast cancer cells.

2.5 | Most cortisol-induced DNA breaks in the G_1 phase are independent of the elongation of RNA synthesis

We explored whether cortisol-induced stalled TOP2ccs occur at transcriptional regulatory sequences or during transcriptional elongation at the gene body. To block the elongation, we added RNA polymerase II inhibitors, 5,6-dichloro-1-β-D ribofuranosylbenzimidazole (DRB) and α-amanitin, 3 h before the exposure of *53BP1*$^{-/-}$/*BRCA1*$^{-/-}$ MCF-7 cells to cortisol (Figure 6a) and confirm the transcription inhibition (Figure S6). We measured γH2AX foci in cyclin-A-negative G_1 cells following serum starvation. The inhibitors only modestly decreased

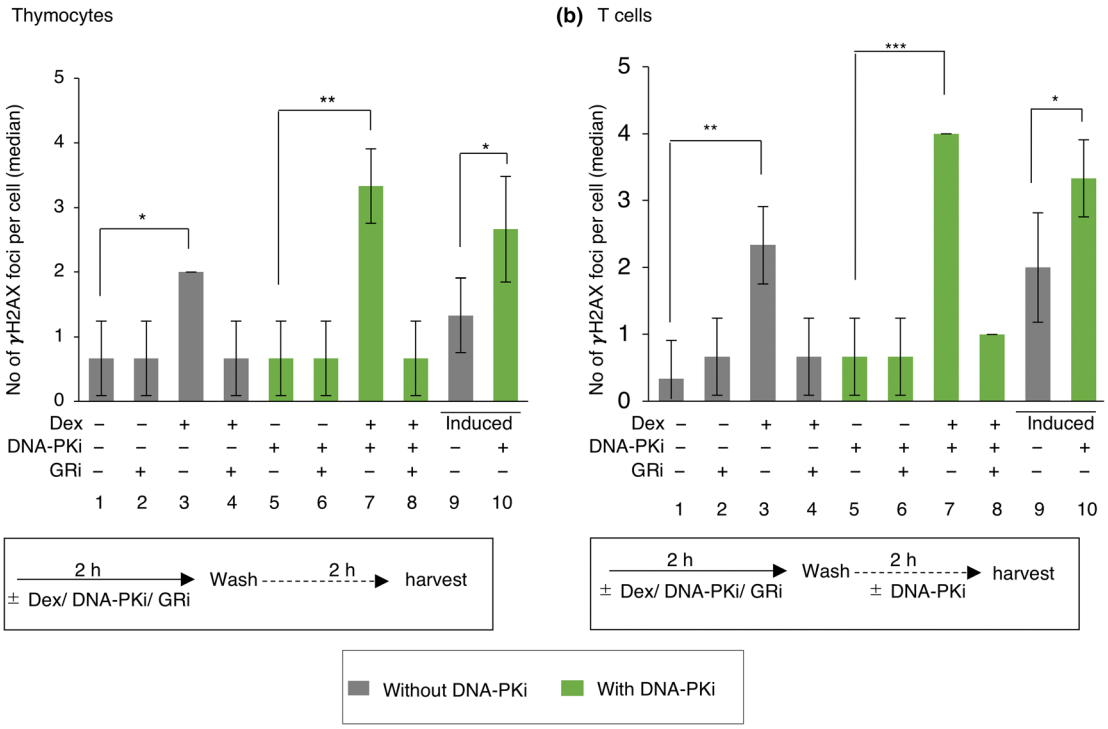

FIGURE 5 Functional GR is required for Dex-induced DSB formation in primary thymocytes and T cells. (a) Mouse primary thymocytes were treated with 10 nM Dex, 10 μM DNA-PKcs inhibitor (DNA-PKi), and 10 μM GR inhibitor (GRi) following the protocol shown at the bottom. The Y-axis is the average median number of γH2AX foci per cell. The average is calculated from the median of three independent experiments. Data of lane 9 (Dex-induced γH2AX foci) was the subtracted value of data of lane 1 from that of lane 3. Data of lane 10 (Dex-induced γH2AX foci in the presence of DNA-PKi) was the subtracted value of data of lane 5 from that of lane 7. The error bar represents the standard deviation (SD) from three independent experiments (100 cells were counted for each replicate). * $p < .05$, ** $p < .01$ (Student's *t*-test). Schematic diagrams of experimental designs are shown in lower panels. See Figure S5 for the distributions of γH2AX focus counts per cell. (b) Mouse primary T cells were treated with 10 nM Dex, 10 μ M DNA-PKi, and 10 μM GRi as shown at the bottom, and data are presented as in Figure 5a. See Figure S5 for the distributions of γH2AX focus counts per cell.

13652443, 0, Downloaded from https://onlinelibrary.wiley.com/doi/10.1111/gtc.12993 by Kyoto University, Wiley Online Library on [14/12/2022]. See the Terms and Conditions (https://onlinelibrary.wiley.com/terms-and-conditions) on Wiley Online Library for rules of use; OA articles are governed by the applicable Creative Commons License

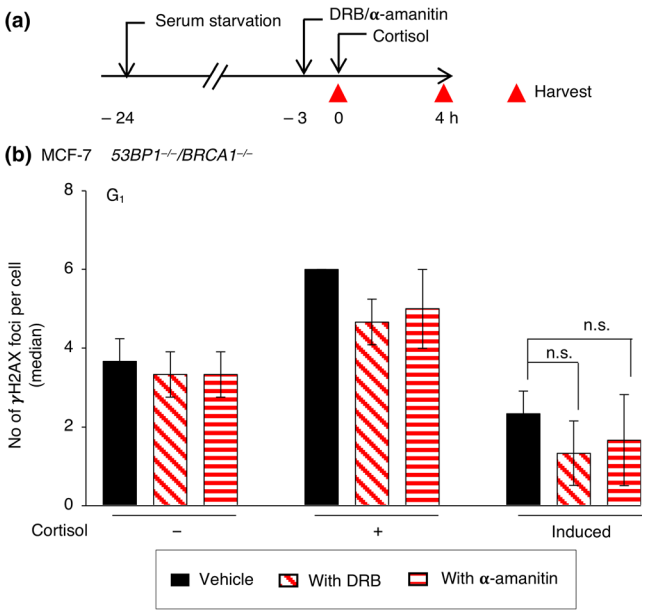

FIGURE 6 Cortisol induces DSBs independently of ongoing transcription in the G_1 phase. (a) Schematic diagram of experimental design to examine the effect of RNA polymerase II inhibitors (DRB and α-amanitin) on cortisol-induced γH2AX-focus formation in 24 h serum starved G_1 arrested cells. Either 25 μM DRB or 100 μM α-amanitin was added to serum-starved *53BP1*$^{-/-}$/*BRCA1*$^{-/-}$ MCF-7 cells 3 h before the addition of cortisol. Red triangles indicate the time points for the analysis of γH2AX foci before or after the addition of cortisol. (b) A modest effect of DRB or α-amanitin on cortisol-induced γH2AX focus formation. The Y-axis is the average of the median number of γH2AX foci per cell. The average is calculated from the median of three independent experiments. The error bar represents the standard deviation (SD) from three independent experiments (100 cells were counted for each replicate). "Induced" indicates the subtracted value of the γH2AX focus number in the absence of treatment with cortisol (−) from that following treatment with cortisol (+). See Figure S6 for the distributions of γH2AX focus counts per cell.

the number of cortisol-induced γH2AX foci (Figure 6b and Figure S6). Thus, most of the GC-induced DSBs are independent of ongoing transcription in the G_1 phase, and this conclusion agrees with the data on the estrogen-induced DSBs (Sasanuma et al., 2018). These observations suggest that stalled TOP2ccs occur at transcriptional regulatory sequences during signal-induced transcription, as previously indicated (Pommier et al., 2016; Puc et al., 2017).

3 | DISCUSSION

We demonstrate that cortisol and Dex induce DSBs by activating GR and generating stalled TOP2ccs in G_0/G_1 cells (Figure 1–5). NHEJ very efficiently seals these DSBs as DSB-repair-proficient cells poorly exhibited GC-induced γH2AX and 53BP1 foci. This conclusion agrees with the fact that GCs do not have any mutagenic potential (Singh et al., 1994). GCs induced stalled TOP2ccs even when the productive elongation of transcription was inhibited before the addition of GCs (Figure 6), indicating that stalled TOP2ccs are formed independently of transcriptional elongation and occur probably at the promoter and enhancer sequences (reviewed in [Pommier et al., 2016; Puc et al., 2017; Pommier et al., 2022]). In conclusion, cortisol and Dex generate many TOP2-dependent DSBs during the transcriptional induction of target genes.

An important question is the number of GC-induced stalled TOP2ccs subjected to the re-ligation by NHEJ. The actual number of GC-induced stalled TOP2ccs may be much higher than the number of γH2AX foci because 5′ TOP2 adducts suppress DNA damage response and the phosphorylation of H2AX (Sciascia et al., 2020). Due to this suppression, we were likely to underestimate the actual number of GC-induced stalled TOP2ccs. Moreover, each prominent γH2AX and 53BP1focus we counted (Figures 1a–d) may consist of many DSBs. This idea is supported by the accumulation of numerous genes activated by GR and estrogen receptors in the subnuclear area, called the phase-separated transcriptional condensate (Boija et al., 2018; Stortz et al., 2020). Thus, each γH2AX and 53BP1 focus may contain multiple GC-induced stalled TOP2ccs. This idea explains why increasing the concentration of cortisol and Dex from 1 nM to 100 nM increased the number of γH2AX foci in primary lymphocytes, only one per cell (Figure 4b,c,e,f). We propose that 100 nM cortisol and 10 nM Dex induce multiple DSBs at phase-separated transcriptional condensates in each cell.

TOP2 catalysis is required for the initiation and productive elongation of transcription. Stalled TOP2ccs forming during early transcriptional response does not occur in the gene body, since the RNA polymerase inhibitors only modestly decreased the number of cortisol-induced γH2AX foci (Figure 6b and Figure S6). Thus, Stalled TOP2ccs are likely to arise at transcriptional regulatory sequences to initiate transcription. Accumulating evidence has demonstrated that stalled TOP2ccs occur at promoters and enhancers during the early transcriptional response to various extracellular stimuli (Álvarez-Quilón et al., 2014; Bunch, 2017; Bunch et al., 2014, 2015; Calderwood, 2016; Haffner et al., 2010; Itou et al., 2020; Ju et al., 2006; Kouzine et al., 2014; Madabhushi et al., 2015; McKinnon, 2016; Miyaji et al., 2020; Sano et al., 2008; Wong et al., 2009) (reviewed in [Pommier et al., 2016, 2022]). Dynamic change of chromatin loop structures ensures physical enhancer-promoter interactions necessary for the early transcriptional

13652443, 0, Downloaded from https://onlinelibrary.wiley.com/doi/10.1111/gtc.12993 by Kyoto University, Wiley Online Library on [14/12/2022]. See the Terms and Conditions (https://onlinelibrary.wiley.com/terms-and-conditions) on Wiley Online Library for rules of use; OA articles are governed by the applicable Creative Commons License

response. Active catalysis of TOP2 is required for this dynamic change (reviewed in [Pommier et al., 2022]). We propose that the active catalysis of TOP2 causes the formation of stalled TOP2ccs at transcriptional regulatory sequences.

Stalled TOP2ccs at transcriptional regulatory sequences can change early transcriptional response when these DSBs are left unrepaired. Because unrepaired stalled TOP2ccs may affect the dynamic change of chromatin loop structures and interfere with the enhancer-promoter interaction. Previous studies documented that TDP2, also called EAPII and TTRAP, is implicated in broad responsiveness to various extracellular signals, including inflammatory cytokines and virus infection (C. Li et al., 2011). It has been postulated that TDP2 directly controls multiple signal transduction pathways, including TNF-TNFR, TGFβ and MAPK, and EAPII, thereby regulating extracellular signal-mediated transcription. Likewise, a previous report documented that DNA-PKcs, a key factor of NHEJ, mediates transcriptional control independent of its function in the DSB repair (Goodwin et al., 2015). However, the current manuscript suggests that the role of TDP2 and DNA-PKcs in DSB repair explains their functioning in signal-mediated transcription and transcriptional control, respectively. Our study suggests that stalled TOP2ccs frequently form most likely at transcriptional regulatory sequences during the early transcriptional response (Figure 6). Thus, TDP2 and DNA-PKcs affect the transcription of genes as the DSB repair factor that acts at transcriptional regulatory sequences. Future studies will reveal the role of DSB repair in transcriptional response to a wide variety of extracellular signals and will uncover molecular mechanisms for the phenotype of many diseases and organ-specific carcinogenesis caused by defective DSB repair. We predict that future studies will also show the genotoxicity of environmental hormones, such as polychlorinated biphenyls (PCB), during transcriptional response.

4 | EXPERIMENTAL PROCEDURES

4.1 | Reagents

All reagents and resources used in this study are listed in Tables S1–S3.

4.2 | Cell culture

MCF-7 cells were maintained in Dulbecco's Modified Eagle Medium (DMEM, Gibco) containing 10% FBS (Gibco), 100 U/ml penicillin, and 100 μg/ml streptomycin (Penicillin–Streptomycin Mixed Solution, Nacalai). TK6 cells were cultured in RPMI1640 medium (Nacalai) supplemented with 5% horse serum (Gibco), 100 U/ml penicillin, and 100 μg/ml streptomycin (Penicillin–Streptomycin Mixed Solution, Nacalai), and 200 mg/ml sodium pyruvate (Thermo Fischer).

4.3 | Mice

Wild-type adult mice (C57BL/6JJmsSIc) were purchased from Shimizu Laboratory Supplies Co., Ltd, Japan. Animal studies were conducted following the institutional guidelines, and experimental procedures were approved by the Animal Experimentation Committee of the Institute for Frontier Life and Medical Sciences, Kyoto University.

4.4 | Generation of *TOP2B*$^{-/-}$/*DNA-PKcs*$^{-/-}$ MCF-7 cells by CRISPR/Cas9-mediated genome-editing

gRNA for the DNA-PKcs gene disruption (Table S3) was designed using the CRISPRdirect software (Naito et al., 2015). The gRNA sequences were inserted into the BbsI site of the pX459 plasmid (Addgene). pX459 expresses gRNA under the control of the U6 promoter and Cas9 under the chicken β-actin promoter. *TOP2B*$^{-/-}$ MCF-7 cells were seeded on a 6 cm dish at around 60% confluency, and the pX459-gRNA was transfected into the cells using Fugene HD (Promega) according to the manufacturer's instructions. Twenty-four hours after the transfection, the cells were treated with puromycin (2 μg/ml) for 48 h. The cells were further incubated in a puromycin-free medium for approximately 2 weeks to isolate single-cell clones. Gene disruption was confirmed by western blotting (Figure S3) using the α-DNA-PKcs antibody (1:200, Abcam ab1832). β-actin was detected as a loading control using the α-β-actin antibody (1:5000, Sigma A5411).

4.5 | Glucocorticoids treatment for immunostaining

MCF-7 cells were arrested in the G_1 phase by 24-h serum starvation in phenol-red-free DMEM (GIBCO) without FBS and subject to glucocorticoid treatment by replacing the medium containing cortisol or dexamethasone. The drugs were directly added to the medium for TK6 cells. After 2 h of the glucocorticoid treatment, cells were washed with PBS and further incubated in a drug-free medium.

13652443, 0, Downloaded from https://onlinelibrary.wiley.com/doi/10.1111/gtc.12993 by Kyoto University, Wiley Online Library on [14/12/2022]. See the Terms and Conditions (https://onlinelibrary.wiley.com/terms-and-conditions) on Wiley Online Library for rules of use; OA articles are governed by the applicable Creative Commons License

Thymuses or lymph nodes were harvested from 3 to 4-week-old *wild-type* male mice, minced into small pieces with scalpel blades, and smashed with the rough surfaces of two slide glasses. The smashed tissues were collected into a falcon tube with RPMI media (RPMI, 10% FBS, 10 mM Hepes buffer pH 7.4, 50 μM beta-mercaptoethanol, 1% penicillin/streptomycin). Cells were passed through 48 μm mesh and centrifuged at 1200 rpm at room temperature for 5 min. After washing with PBS, cells were treated with glucocorticoids and incubated in RPMI medium in a humidified CO_2 incubator at 37°C. Two hours after the treatment, cells were washed with PBS a few times, incubated in a drug-free medium, and harvested at different time points for immunostaining.

4.6 | Immunostaining

MCF-7 cells cultured on coverslips were fixed with cold methanol for 20 min on ice. TK6 cells were spun onto a slide using Cytospin (Shandon, Pittsburgh), followed by fixation with formaldehyde (4% in PBS) at room temperature for 10 min. Cells were permeabilized with 0.5% Triton X-100 in PBS for 10 min, followed by blocking with PBS containing 5% BSA (1% BSA for MCF-7 γH2AX staining) at room temperature for an hour. Primary antibody incubation was performed at room temperature for an hour or 4°C overnight using α-γH2AX (1:1000, Millipore 05–636) and α-cyclin A (1:500, Santa Cruz sc-596), or α-53BP1 (1:1000, Calbiochem PC712) and α-cyclin A (1:500, Santa Cruz sc-271,682). Cells were washed with PBS three times and stained with the α-mouse Alexa Fluor 488 antibody (1:1000, Thermo Fisher Scientific A-11029) and the α-rabbit Alexa Fluor 594 antibody (1:1000, Thermo Fisher Scientific A11037) at room temperature for an hour. Slides were washed with PBS three times and mounted in Fluoro-KEEPER containing 4, 6-diamidino-2-phenylindole (DAPI) (Nacalai).

Mouse primary cells were spun onto a slide using Cytospin, fixed with 4% paraformaldehyde in PBS at room temperature for 10 min, and washed with TPBS washing buffer (1% BSA, 0.05% Tween-20 in PBS) three times. Cells were then blocked with TPBS-Triton buffer (1% BSA, 0.2% Triton X-100, 5%–10% FBS in PBS) for 1–2 h. Primary antibody incubation was performed in TPBS-Triton buffer at room temperature for an hour (or at 4°C overnight) using α-γH2AX (1:500, Cell Signaling 9718) and APC-conjugated α-mouse CD3ε (1:50, BD Pharmingen 553,066). Slides were washed with TPBS buffer and incubated with the α-rabbit Alexa Fluor 488 antibody (1:1000, Thermo Fisher A-11034) in TPBS-Triton buffer. Slides were washed with TPBS and mounted as described above. The immunofluorescence image was captured using a BZ-9000 fluorescence microscope (KEYENCE). Nuclear foci in at least 100 cells were counted manually for each biological replicate.

4.7 | Chromosome aberration analysis in mitotic chromosome spreads

MCF-7 cells were cultured in the phenol red-free DMEM medium containing 5% charcoal-stripped FBS (Hyclone SH30068.03) for 24 h, followed by a 36-h treatment with 100 nM cortisol or 10 nM or 100 nM dexamethasone. TK6 cells were treated with 100 nM cortisol or 10 nM dexamethasone in RPMI medium for 15 h. Chromosome aberration analysis was performed as described previously (Hoa et al., 2015). Briefly, cells exposed to glucocorticoids were treated with 0.1 μg/ml of colcemid (Thermo Fischer) for 3 h. Cells were then incubated in 75 mM of potassium chloride for 15 min, washed with Carnoy's solution (3:1 mixture of methanol and acetic acid), incubated with Carnoy's solution for at least 1 hr, dropped on slides, and stained with 5% Giemsa solution for 10 min. Slides were washed with PBS and mounted with MX oil (Matsunami Glass Industry).

4.8 | Western blotting

One million cells were lysed in 100 μl sodium dodecyl sulfate (SDS) buffer, containing 25 mM Tris–HCl (pH 6.5), 1% SDS, 0.24 mM β-mercaptoethanol, 0.1% bromophenol blue and 5% glycerol. The whole-cell extracts were separated by electrophoresis and transferred onto polyvinylidene difluoride membranes. Membranes were blocked in 5% skimmed milk in TBS-T (0.1% Tween-20 in TBS) and incubated with primary antibodies overnight at 4°C. The membranes were washed with TBS-T and incubated with appropriate HRP-linked secondary antibodies at room temperature for an hour. Following the TBS-T wash, the chemiluminescence signal was detected using ECL reagents.

4.9 | EU incorporation

Cells were labeled with EU (1 mM) for 2 h and fixed with paraformaldehyde (4%) for 10 min at room temperature. After permeabilization with Triton X-100/1X PBS (0.5%) for 20 min at room temperature. Stained with 100 mM Tris HCl, pH 8.5,1 mM CuSO4, 1 μM Alexa fluor 647 azide, freshly prepared 100 mM ascorbic acid (added last from 0.5 M stock in water) for 30 min at room temperature, protected from light as described previously

13652443, 0, Downloaded from https://onlinelibrary.wiley.com/doi/10.1111/gtc.12993 by Kyoto University, Wiley Online Library on [14/12/2022]. See the Terms and Conditions (https://onlinelibrary.wiley.com/terms-and-conditions) on Wiley Online Library for rules of use; OA articles are governed by the applicable Creative Commons License

(Jao & Salic, 2008). Samples were mounted with Vectashield containing DAPI and imaged using a BZ-9000 (KEYENCE, Japan) using a 100X objective lens.

4.10 | Quantification and statistical analysis

For statistical analyses with *p*-values, unpaired Student's *t*-test was used for the main figures, and Mann–Whitney U test was used for the supplementary figures. The error bar represents the standard deviation (SD), as indicated in the legends. *p*-values were calculated using at least three biological replicates.

AUTHOR CONTRIBUTIONS

Salma Akter performed the majority of the experiments; Akihiro Shimba did animal experiments; Md. Rasel Al Mahmud, Hiroyuki Sasanuma, Masataka Tsuda, Masakatsu Sone, Yukio Ago, and Kenichi Murai performed and evaluated individual experiments; Shunichi Takeda and Shintaro Yamada designed and supervised individual experiments; Salma Akter and Shunichi Takeda wrote the manuscript with the contributions from all the authors.

ACKNOWLEDGMENTS

We thank the members of the Radiation Genetics laboratory at Kyoto University and all the co-authors. This work was supported by JSPS KAKENHI (19 K20449 and 21 K07148), Fujiwara Memorial Foundation, the Takeda Science Foundation (to SY), JSPS KAKENHI (18H03992 and 20KK0186), JSPS KAKENHI (20 K21525) (to KI), JSPS KAKENHI (20 K16280) (to AS), JSPS KAKENHI (16H12595 and 16H06306) (to ST), the JSPS Core-to-Core Program, A. Advanced Research Networks (to ST) and by JSPS KAKENHI (19H04267) (to HS). We also thank the technical support provided by Prof. Masatoshi Hagiwara and the Medical Research Support Center of Kyoto University. The authors acknowledge Dr. Hisashi Tanaka (Cedar-Sinai hospital, LA, USA), Dr. Soonjoung Kim, and David Ontoso (Memorial Sloan Kettering Cancer Center, NY, USA) for critical reading.

CONFLICT OF INTEREST

The authors declare no competing financial interests.

ORCID

Hiroyuki Sasanuma https://orcid.org/0000-0003-2824-4499
Shunichi Takeda https://orcid.org/0000-0002-7924-7991

REFERENCES

Akagawa, R., Trinh, H. T., Saha, L. K., Tsuda, M., Hirota, K., Yamada, S., Shibata, A., Kanemaki, M. T., Nakada, S., Takeda, S., & Sasanuma, H. (2020). UBC13-mediated ubiquitin signaling promotes removal of blocking adducts from DNA double-Strand breaks. *IScience*, *23*(4), 101027. https://doi.org/10.1016/j.isci.2020.101027

Al Mahmud, M. R., Ishii, K., Bernal-Lozano, C., Delgado-Sainz, I., Toi, M., Akamatsu, S., Fukumoto, M., Watanabe, M., Takeda, S., Ledesma, F. C., & Sasanuma, H. (2020). TDP2 suppresses genomic instability induced by androgens in the epithelial cells of prostate glands. *Genes to Cells: Devoted to Molecular & Cellular Mechanisms*, *25*(7), 450–465. https://doi.org/10.1111/gtc.12770

Álvarez-Quilón, A., Serrano-Benítez, A., Ariel Lieberman, J., Quintero, C., Sánchez-Gutiérrez, D., Escudero, L. M., & Cortés-Ledesma, F. (2014). ATM specifically mediates repair of double-strand breaks with blocked DNA ends. *Nature Communications*, *5*, 3347. https://doi.org/10.1038/ncomms4347

Austin, C. A., Lee, K. C., Swan, R. L., Khazeem, M. M., Manville, C. M., Cridland, P., Treumann, A., Porter, A., Morris, N. J., & Cowell, I. G. (2018). TOP2B: The first thirty years. *International Journal of Molecular Sciences*, *19*(9), 2765. https://doi.org/10.3390/ijms19092765

Boija, A., Klein, I. A., Sabari, B. R., Dall'Agnese, A., Coffey, E. L., Zamudio, A. V., Li, C. H., Shrinivas, K., Manteiga, J. C., Hannett, N. M., Abraham, B. J., Afeyan, L. N., Guo, Y. E., Rimel, J. K., Fant, C. B., Schuijers, J., Lee, T. I., Taatjes, D. J., & Young, R. A. (2018). Transcription factors activate genes through the phase-separation capacity of their activation domains. *Cell*, *175*(7), 1842–1855.e16. https://doi.org/10.1016/j.cell.2018.10.042

Buick, J. K., Moffat, I., Williams, A., Swartz, C. D., Recio, L., Hyduke, D. R., Li, H. H., Fornace, A. J., Jr., Aubrecht, J., & Yauk, C. L. (2015). Integration of metabolic activation with a predictive toxicogenomics signature to classify genotoxic versus nongenotoxic chemicals in human TK6 cells. *Environmental and Molecular Mutagenesis*, *56*(6), 520–534. https://doi.org/10.1002/em.21940

Bunch, H. (2017). RNA polymerase II pausing and transcriptional regulation of the HSP70 expression. *European Journal of Cell Biology*, *96*(8), 739–745. https://doi.org/10.1016/j.ejcb.2017.09.003

Bunch, H., Zheng, X., Burkholder, A., Dillon, S. T., Motola, S., Birrane, G., Ebmeier, C. C., Levine, S., Fargo, D., Hu, G., Taatjes, D. J., & Calderwood, S. K. (2014). TRIM28 regulates RNA polymerase II promoter-proximal pausing and pause release. *Nature Structural & Molecular Biology*, *21*(10), 876–883. https://doi.org/10.1038/nsmb.2878

Bunch, H., Lawney, B. P., Lin, Y.-F., Asaithamby, A., Murshid, A., Wang, Y. E., Chen, B. P., & Calderwood, S. K. (2015). Transcriptional elongation requires DNA break-induced signalling. *Nature Communications*, *6*, 10191. https://doi.org/10.1038/ncomms10191

Cain, D. W., & Cidlowski, J. A. (2020). After 62 years of regulating immunity, dexamethasone meets COVID-19. *Nature Reviews. Immunology*, *20*(10), 587–588. https://doi.org/10.1038/s41577-020-00421-x

Calderwood, S. K. (2016). A critical role for topoisomerase IIb and DNA double strand breaks in transcription. *Transcription*, *7*(3), 75–83. https://doi.org/10.1080/21541264.2016.1181142

13652443, 0, Downloaded from https://onlinelibrary.wiley.com/doi/10.1111/gtc.12993 by Kyoto University, Wiley Online Library on [14/12/2022]. See the Terms and Conditions (https://onlinelibrary.wiley.com/terms-and-conditions) on Wiley Online Library for rules of use; OA articles are governed by the applicable Creative Commons License

Canela, A., Maman, Y., Huang, S.-Y. N., Wutz, G., Tang, W., Zagnoli-Vieira, G., Callen, E., Wong, N., Day, A., Peters, J. M., Caldecott, K. W., Pommier, Y., & Nussenzweig, A. (2019). Topoisomerase II-induced chromosome breakage and translocation is determined by chromosome architecture and transcriptional activity. *Molecular Cell*, *75*(2), 252–266.e8. https://doi.org/10.1016/j.molcel.2019.04.030

Chappell, C. (2002). Involvement of human polynucleotide kinase in double-strand break repair by non-homologous end joining. *The EMBO Journal*, *21*(11), 2827–2832. https://doi.org/10.1093/emboj/21.11.2827

Fellows, M. D., & O'Donovan, M. R. (2010). Etoposide, cadmium chloride, benzo[a]pyrene, cyclophosphamide and colchicine tested in the in vitro mammalian cell micronucleus test (MNvit) in the presence and absence of cytokinesis block using L5178Y mouse lymphoma cells and 2-aminoanthracene tested in MNvit in the absence of cytokinesis block using TK6 cells at AstraZeneca UK, in support of OECD draft test guideline 487. *Mutation Research*, *702*(2), 163–170. https://doi.org/10.1016/j.mrgentox.2009.09.003

Ghosh, D., & Raghavan, S. C. (2021). Nonhomologous end joining: New accessory factors fine tune the machinery. *Trends in Genetics: TIG*, *37*(6), 582–599. https://doi.org/10.1016/j.tig.2021.03.001

Gollapudi, B. B., White, P. A., & Honma, M. (2019). The IWGT in vitro mammalian cell gene mutation (MCGM) assays working group-introductory remarks & consensus statements. *Mutation Research*, *848*, 403061. https://doi.org/10.1016/j.mrgentox.2019.05.017

Gómez-Herreros, F., Schuurs-Hoeijmakers, J. H. M., McCormack, M., Greally, M. T., Rulten, S., Romero-Granados, R., Counihan, T. J., Chaila, E., SCJ, E., Delanty, N., Cortes-Ledesma, F., de Brouwer, A. P., Cavalleri, G. L., El-khamisy, S. F., de Vries, B. B., & Caldecott, K. W. (2014). TDP2 protects transcription from abortive topoisomerase activity and is required for normal neural function. *Nature Genetics*, *46*(5), 516–521. https://doi.org/10.1038/ng.2929

Goodwin, J. F., Kothari, V., Drake, J. M., Zhao, S., Dylgjeri, E., Dean, J. L., Schiewer, M. J., McNair, C., Jones, J. K., Aytes, A., Magee, M. S., Snook, A. E., Zhu, Z., Den RB, B. R. C., Gomella, L. G., Graham, N. A., Vashisht, A. A., Wohlschlegel, J. A., Graeber, T. G., … Knudsen, K. E. (2015). DNA-PKcs-mediated transcriptional regulation drives prostate cancer progression and metastasis. *Cancer Cell*, *28*(1), 97–113. https://doi.org/10.1016/j.ccell.2015.06.004

Guess, A., Agrawal, S., Wei, C.-C., Ransom, R. F., Benndorf, R., & Smoyer, W. E. (2010). Dose- and time-dependent glucocorticoid receptor signaling in podocytes. *American Journal of Physiology. Renal Physiology*, *299*(4), F845–F853. https://doi.org/10.1152/ajprenal.00161.2010

Haffner, M. C., Aryee, M. J., Toubaji, A., Esopi, D. M., Albadine, R., Gurel, B., Isaacs, W. B., Bova, G. S., Liu, W., Xu, J., Meeker, A. K., Netto, G., AMD, M., Nelson, W. G., & Yegnasubramanian, S. (2010). Androgen-induced TOP2B-mediated double-strand breaks and prostate cancer gene rearrangements. *Nature Genetics*, *42*(8), 668–675. https://doi.org/10.1038/ng.613

Heming, N., Sivanandamoorthy, S., Meng, P., Bounab, R., & Annane, D. (2018). Immune effects of corticosteroids in sepsis. *Frontiers in Immunology*, *9*, 1736. https://doi.org/10.3389/fimmu.2018.01736

Hoa, N. N., Kobayashi, J., Omura, M., Hirakawa, M., Yang, S.-H., Komatsu, K., Paull, T. T., Takeda, S., & Sasanuma, H. (2015). BRCA1 and CtIP are both required to recruit Dna2 at double-Strand breaks in homologous recombination. *PLoS One*, *10*(4), e0124495. https://doi.org/10.1371/journal.pone.0124495

Hoa, N. N., Shimizu, T., Zhou, Z. W., Wang, Z.-Q., Deshpande, R. A., Paull, T. T., Akter, S., Tsuda, M., Furuta, R., Tsutsui, K., Takeda, S., & Sasanuma, H. (2016). Mre11 is essential for the removal of lethal topoisomerase 2 covalent cleavage complexes. *Molecular Cell*, *64*(5), 1010. https://doi.org/10.1016/j.molcel.2016.11.028

Huang, W., Kalhorn, T. F., Baillie, M., Shen, D. D., & Thummel, K. E. (2007). Determination of free and total cortisol in plasma and urine by liquid chromatography-tandem mass spectrometry. *Therapeutic Drug Monitoring*, *29*(2), 215–224. https://doi.org/10.1097/FTD.0b013e31803d14c0

Itou, J., Takahashi, R., Sasanuma, H., Tsuda, M., Morimoto, S., Matsumoto, Y., Ishii, T., Sato, F., Takeda, S., & Toi, M. (2020). Estrogen induces mammary ductal dysplasia via the upregulation of Myc expression in a DNA-repair-deficient condition. *IScience*, *23*(2), 100821. https://doi.org/10.1016/j.isci.2020.100821

Jao, C. Y., & Salic, A. (2008). Exploring RNA transcription and turnover in vivo by using click chemistry. *Proceedings of the National Academy of Sciences of the United States of America*, *105*(41), 15779–15784. https://doi.org/10.1073/pnas.0808480105

Joshi, R. S., Piña, B., & Roca, J. (2012). Topoisomerase II is required for the production of long pol II gene transcripts in yeast. *Nucleic Acids Research*, *40*(16), 7907–7915. https://doi.org/10.1093/nar/gks626

Ju, B.-G., Lunyak, V. V., Perissi, V., Garcia-Bassets, I., Rose, D. W., Glass, C. K., & Rosenfeld, M. G. (2006). *A topoisomerase IIbeta-mediated dsDNA break required for regulated transcription*. New York, N.Y: Science (Vol. 312, pp. 1798–1802). https://doi.org/10.1126/science.1127196

Karras, G. I., Yi, S., Sahni, N., Fischer, M., Xie, J., Vidal, M., D'Andrea, A. D., Whitesell, L., & Lindquist, S. (2017). HSP90 shapes the consequences of human genetic variation. *Cell*, *168*(5), 856–866.e12. https://doi.org/10.1016/j.cell.2017.01.023

King, I. F., Yandava, C. N., Mabb, A. M., Hsiao, J. S., Huang, H.-S., Pearson, B. L., Calabrese, J. M., Starmer, J., Parker, J. S., Magnuson, T., Chamberlain, S. J., Philpot, B. D., & Zylka, M. J. (2013). Topoisomerases facilitate transcription of long genes linked to autism. *Nature*, *501*(7465), 58–62. https://doi.org/10.1038/nature12504

Kouzine, F., Levens, D., & Baranello, L. (2014). DNA topology and transcription. *Nucleus (Austin, Tex.)*, *5*(3), 195–202. https://doi.org/10.4161/nucl.28909

Lai, C.-H., Park, K.-S., Lee, D.-H., Alberobello, A. T., Raffeld, M., Pierobon, M., Pin, E., Petricoin, E. F., Wang, Y., & Giaccone, G. (2014). HSP-90 inhibitor ganetespib is synergistic with doxorubicin in small cell lung cancer. *Oncogene*, *33*(40), 4867–4876. https://doi.org/10.1038/onc.2013.439

Ledesma, F. C., El Khamisy, S. F., Zuma, M. C., Osborn, K., & Caldecott, K. W. (2009). A human 5′-tyrosyl DNA phosphodiesterase that repairs topoisomerase-mediated DNA damage. *Nature*, *461*(7264), 674–678. https://doi.org/10.1038/nature08444

13652443, 0, Downloaded from https://onlinelibrary.wiley.com/doi/10.1111/gtc.12993 by Kyoto University, Wiley Online Library on [14/12/2022]. See the Terms and Conditions (https://onlinelibrary.wiley.com/terms-and-conditions) on Wiley Online Library for rules of use; OA articles are governed by the applicable Creative Commons License

Li, C., Sun, S.-Y., Khuri, F. R., & Li, R. (2011). Pleiotropic functions of EAPII/TTRAP/TDP2: Cancer development, chemoresistance and beyond. *Cell Cycle (Georgetown, Tex.)*, *10*(19), 3274–3283. https://doi.org/10.4161/cc.10.19.17763

Li, H.-H., Chen, R., Hyduke, D. R., Williams, A., Frötschl, R., Ellinger-Ziegelbauer, H., O'Lone, R., Yauk, C. L., Aubrecht, J., & Fornace, A. J. (2017). Development and validation of a high-throughput transcriptomic biomarker to address 21st century genetic toxicology needs. *Proceedings of the National Academy of Sciences of the United States of America*, *114*(51), E10881–E10889. https://doi.org/10.1073/pnas.1714109114

Madabhushi, R. (2018). The roles of DNA topoisomerase IIβ in transcription. *International Journal of Molecular Sciences*, *19*(7), 1917. https://doi.org/10.3390/ijms19071917

Madabhushi, R., Gao, F., Pfenning, A. R., Pan, L., Yamakawa, S., Seo, J., Rueda, R., Phan, T. X., Yamakawa, H., Pao, P. C., Stott, R. T., Gjoneska, E., Nott, A., Cho, S., Kellis, M., & Tsai, L.-H. (2015). Activity-induced DNA breaks govern the expression of neuronal early-response genes. *Cell*, *161*(7), 1592–1605. https://doi.org/10.1016/j.cell.2015.05.032

McKinnon, P. J. (2016). Topoisomerases and the regulation of neural function. *Nature Reviews Neuroscience*, *17*(11), 673–679. https://doi.org/10.1038/nrn.2016.101

Miyaji, M., Furuta, R., Hosoya, O., Sano, K., Hara, N., Kuwano, R., Kang, J., Tateno, M., Tsutsui, K. M., & Tsutsui, K. (2020). Topoisomerase IIβ targets DNA crossovers formed between distant homologous sites to induce chromatin opening. *Scientific Reports*, *10*(1), 18550. https://doi.org/10.1038/s41598-020-75004-w

Morgan, B. P., Swick, A. G., Hargrove, D. M., LaFlamme, J. A., Moynihan, M. S., Carroll, R. S., Martin, K. A., Lee, E., Decosta, D., & Bordner, J. (2002). Discovery of potent, nonsteroidal, and highly selective glucocorticoid receptor antagonists. *Journal of Medicinal Chemistry*, *45*(12), 2417–2424. https://doi.org/10.1021/jm0105530

Morimoto, S., Tsuda, M., Bunch, H., Sasanuma, H., Austin, C., & Takeda, S. (2019). Type II DNA topoisomerases cause spontaneous double-Strand breaks in genomic DNA. *Genes*, *10*(11), 868. https://doi.org/10.3390/genes10110868

Naito, Y., Hino, K., Bono, H., & Ui-Tei, K. (2015). CRISPRdirect: Software for designing CRISPR/Cas guide RNA with reduced off-target sites. *Bioinformatics*, *31*(7), 1120–1123. https://doi.org/10.1093/bioinformatics/btu743

Nitiss, J. L. (2009). Targeting DNA topoisomerase II in cancer chemotherapy. *Nature Reviews. Cancer*, *9*(5), 338–350. https://doi.org/10.1038/nrc2607

Pommier, Y., Sun, Y., Huang, S. N., & Nitiss, J. L. (2016). Roles of eukaryotic topoisomerases in transcription, replication and genomic stability. *Nature Reviews Molecular Cell Biology*, *17*(11), 703–721. https://doi.org/10.1038/nrm.2016.111

Pommier, Y., Nussenzweig, A., Takeda, S., & Austin, C. (2022). Human topoisomerases and their roles in genome stability and organization. *Nature Reviews. Molecular Cell Biology*, *23*(6), 407–427. https://doi.org/10.1038/s41580-022-00452-3

Puc, J., Aggarwal, A. K., & Rosenfeld, M. G. (2017). Physiological functions of programmed DNA breaks in signal-induced transcription. *Nature Reviews. Molecular Cell Biology*, *18*(8), 471–476. https://doi.org/10.1038/nrm.2017.43

Robins, P., & Lindahl, T. (1996). DNA ligase IV from HeLa cell nuclei. *Journal of Biological Chemistry*, *271*(39), 24257–24261. https://doi.org/10.1074/jbc.271.39.24257

Russell, G., & Lightman, S. (2019). The human stress response. *Nature Reviews. Endocrinology*, *15*(9), 525–534. https://doi.org/10.1038/s41574-019-0228-0

Sano, K., Miyaji-Yamaguchi, M., Tsutsui, K. M., & Tsutsui, K. (2008). Topoisomerase IIbeta activates a subset of neuronal genes that are repressed in AT-rich genomic environment. *PLoS One*, *3*(12), e4103. https://doi.org/10.1371/journal.pone.0004103

Sasanuma, H., Tsuda, M., Morimoto, S., Saha, L. K., Rahman, M. M., Kiyooka, Y., Fujiike, H., Cherniack, A. D., Itou, J., Moreu, E. C., Toi, M., Nakada, S., Tanaka, H., Tsutsui, K., Yamada, S., Nussenzweig, A., & Takeda, S. (2018). BRCA1 ensures genome integrity by eliminating estrogen-induced pathological topoisomerase II–DNA complexes. *Proceedings of the National Academy of Sciences*, *115*(45), E10642–E10651. https://doi.org/10.1073/pnas.1803177115

Scheer, F. A. J. L., Van Paassen, B., Van Montfrans, G. A., Fliers, E., Van Someren, E. J. W., Van Heerikhuize, J. J., & Buijs, R. M. (2002). Human basal cortisol levels are increased in hospital compared to home setting. *Neuroscience Letters*, *333*(2), 79–82. https://doi.org/10.1016/S0304-3940(02)00988-6

Sciascia, N., Wu, W., Zong, D., Sun, Y., Wong, N., John, S., Wangsa, D., Ried, T., Bunting, S. F., Pommier, Y., & Nussenzweig, A. (2020). Suppressing proteasome mediated processing of topoisomerase II DNA-protein complexes preserves genome integrity. *eLife*, *9*, e53. https://doi.org/10.7554/eLife.53447

Singh, H., Singh, J. R., Dhillon, V. S., Bali, D., & Paul, H. (1994). In vitro and in vivo genotoxicity evaluation of hormonal drugs II. Dexamethasone. *Mutation Research*, *308*(1), 89–97. https://doi.org/10.1016/0027-5107(94)90201-1

Spoorenberg, S. M. C., Deneer, V. H. M., Grutters, J. C., Pulles, A. E., Voorn, G. P. P., Rijkers, G. T., WJW, B., & van de Garde, E. M. W. (2014). Pharmacokinetics of oral vs. intravenous dexamethasone in patients hospitalized with community-acquired pneumonia. *British Journal of Clinical Pharmacology*, *78*(1), 78–83. https://doi.org/10.1111/bcp.12295

Stortz, M., Pecci, A., Presman, D. M., & Levi, V. (2020). Unraveling the molecular interactions involved in phase separation of glucocorticoid receptor. *BMC Biology*, *18*(1), 59. https://doi.org/10.1186/s12915-020-00788-2

Strehl, C., Ehlers, L., Gaber, T., & Buttgereit, F. (2019). Glucocorticoids-all-Rounders tackling the versatile players of the immune system. *Frontiers in Immunology*, *10*, 1744. https://doi.org/10.3389/fimmu.2019.01744

Tubbs, A., & Nussenzweig, A. (2017). Endogenous DNA damage as a source of genomic instability in cancer. *Cell*, *168*(4), 644–656. https://doi.org/10.1016/j.cell.2017.01.002

Weijtens, O., Schoemaker, R. C., Cohen, A. F., Romijn, F. P., Lentjes, E. G., van Rooij, J., & van Meurs, J. C. (1998). Dexamethasone concentration in vitreous and serum after oral administration. *American Journal of Ophthalmology*, *125*(5), 673–679. https://doi.org/10.1016/s0002-9394(98)00003-8

Wong, R. H. F., Chang, I., Hudak, C. S. S., Hyun, S., Kwan, H.-Y., & Sul, H. S. (2009). A role of DNA-PK for the metabolic gene

13652443, 0, Downloaded from https://onlinelibrary.wiley.com/doi/10.1111/gtc.12993 by Kyoto University, Wiley Online Library on [14/12/2022]. See the Terms and Conditions (https://onlinelibrary.wiley.com/terms-and-conditions) on Wiley Online Library for rules of use; OA articles are governed by the applicable Creative Commons License

regulation in response to insulin. *Cell*, *136*(6), 1056–1072. https://doi.org/10.1016/j.cell.2008.12.040

Yauk, C. L., Buick, J. K., Williams, A., Swartz, C. D., Recio, L., Li, H.-H., Fornace, A. J., Jr., Thomson, E. M., & Aubrecht, J. (2016). Application of the TGx-28.65 transcriptomic biomarker to classify genotoxic and non-genotoxic chemicals in human TK6 cells in the presence of rat liver S9. *Environmental and Molecular Mutagenesis*, *57*(4), 243–260. https://doi.org/10.1002/em.22004

Yu, T., MacPhail, S. H., Banáth, J. P., Klokov, D., & Olive, P. L. (2006). Endogenous expression of phosphorylated histone H2AX in tumors in relation to DNA double-strand breaks and genomic instability. *DNA Repair*, *5*(8), 935–946. https://doi.org/10.1016/j.dnarep.2006.05.040

SUPPORTING INFORMATION

Additional supporting information can be found online in the Supporting Information section at the end of this article.

How to cite this article: Akter, S., Shimba, A., Ikuta, K., Mahmud, M. R. A., Yamada, S., Sasanuma, H., Tsuda, M., Sone, M., Ago, Y., Murai, K., Tanaka, H., & Takeda, S. (2022). Physiological concentrations of glucocorticoids induce pathological DNA double-strand breaks. *Genes to Cells*, 1–15. https://doi.org/10.1111/gtc.12993

13652443, 0, Downloaded from https://onlinelibrary.wiley.com/doi/10.1111/gtc.12993 by Kyoto University, Wiley Online Library on [14/12/2022]. See the Terms and Conditions (https://onlinelibrary.wiley.com/terms-and-conditions) on Wiley Online Library for rules of use; OA articles are governed by the applicable Creative Commons License